Synthesis and characterisation of zinc hydroxides nitrates–sodium dodecyl sulphate fluazinam nano hosts for release properties

by Rahadian Zainul Et.al

Submission date: 20-May-2021 02:04PM (UTC+0700)
Submission ID: 1590149767
File name: Ok_Paper_terbaru_Jurnal_Porous_1.pdf (690.54K)
Word count: 8551
Character count: 38913

Synthesis and characterisation of zinc hydroxides nitrates–sodium dodecyl sulphate fluazinam nano hosts for release properties

Hani Masitah MadJin, Norhayati Hashim, Illyas Md Isa, Mohd Zobir Hussein, Suriani Abu Bakar, Mazidah Mamat, Rozita Ahmad, et al.

Journal of Porous Materials

ISSN 1380-2224

J Porous Mater
DOI 10.1007/s10934-020-00925-w

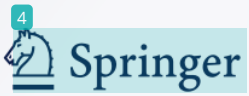

Journal of Porous Materials
https://doi.org/10.1007/s10934-020-00925-w

Synthesis and characterisation of zinc hydroxides nitrates–sodium dodecyl sulphate fluazinam nano hosts for release properties

Hani Masitah MadJin[1] · Norhayati Hashim[1,2] · Illyas Md Isa[1,2] · Mohd Zobir Hussein[3] · Suriani Abu Bakar[2,4] · Mazidah Mamat[5] · Rozita Ahmad[6] · Rahadian Zainul[7]

Abstract
A new nano host-fungicide, namely zinc hydroxide nitrate–sodium dodecyl sulphate–fluazinam (ZHN–SDS–FZ) was successfully synthesised using an ion exchange method. The intercalation of fluazinam (FZ) in the interlayer gallery of ZHN–SDS was confirmed by PXRD pattern with the basal spacing of 32.7 Å. The FTIR confirmed that FZ exist in the interlayer gallery. The elemental analysis also supported the presence of FZ in the interlayer ZHN–SDS where the percentages of nitrogen, which contributed by FZ was 65.6%. Meanwhile, the percentages of Zn in the nano host-fungicides was estimated to be 11.5%. Furthermore, TGA/DTG pattern showed that the nano host-fungicide ZHN–SDS–FZ has better thermal stability compared to pure FZ. The intercalation of FZ leads to the change of morphology, surface area and also the porosity. The classification of porosity of ZHN–SDS is mesoporous, meanwhile ZHN–SDS–FZ is non-porous. The BET-BJH surface area shows that ZHN–SDS and ZHN–SDS–FZ is of Type IV and Type III respectively. The controlled release of FZ from the ZHN–SDS–FZ nano host showed that phosphate and carbonate solutions yield the higher percentages of release compared to chloride solutions. The controlled release of FZ was found to be governed by a pseudo-second order mechanism for all medium. In this research, FZ can act as a good guest anion to be intercalated in the interlayer ZHN–SDS to be further used in agricultural sector due to the slowest release of FZ in the phosphate, carbonate and chloride solutions as a release medium.

Keywords Nano host · Fluazinam · Sodium dodecyl sulphate · Zinc hydroxides nitrate · Release

✉ Norhayati Hashim
norhayati.hashim@fsmt.upsi.edu.my

1 Department of Chemistry, Faculty of Science and Mathematics, Universiti Pendidikan Sultan Idris, 35900 Tanjong Malim, Perak, Malaysia

2 Nanotechnology Research Centre, Faculty of Science and Mathematics, Universiti Pendidikan Sultan Idris, 35900 Tanjong Malim, Perak, Malaysia

3 Materials Synthesis and Characterisation Laboratory, Institute of Advanced Technology, Universiti Putra Malaysia, 43400 Serdang, Selangor, Malaysia

4 Department of Physics, Faculty of Science and Mathematics, Universiti Pendidikan Sultan Idris, 35900 Tanjong Malim, Perak, Malaysia

5 Pusat Pengajian Sains Asas, Universiti Malaysia Terengganu, 21030 Kuala Terengganu, Terengganu, Malaysia

6 Forest Biotechnology Division, Forest Research Institute Malaysia, 52109 Kepong, Selangor, Malaysia

7 Department of Chemistry, Faculty of Mathematics and Natural Science, Universitas Negeri Padang, Padang, West Sumatera 25171, Indonesia

1 Introduction

Layered inorganic materials for an example layered hydroxide salt (LHS) and layered double hydroxide (LDH) enables to intercalate the great anion that compatible in the interlayer space that provide great attention as platform for an intercalated to form new layered materials [1]. Layered materials are defined as a crystalline materials in which the interlayer atoms are bonded with various bonds such as covalent, ionic, ion covalent and metallic bonds [2]. Layered metal hydroxides such as $(Zn(OH)_2)$ is the simplest examples of compounds that comes from brucite-like structures. The brucite-like structure can undergo the substitution of a part hydroxide group by water molecules and anions. It was same characteristic with layered hydroxides salts (LHSs) that consists of a positively charge metal hydroxides nanolayer and interlayer anions which consist of exchange anions and water molecules [3]. Lately, layered materials are often used that act as host matrices for many guest anions for an example, ferric chloride [4],

P-coumaric acid (pCA) [5], nucleotides and DNA [6], ferulic acid (FA) [7], chlorpyrifos [8], cyclamate and saccharin [9], ethylenediaminetetraacetate (EDTA) [10], 4-chlorophenoxyacetate [11], ciprofloxacin [12], dodecylsulfate (DDS) and dodecyl benzenesulfonate (DBS) [13], L-phenylalanate [14], and hexaconazole [15].

For zinc hydroxide nitrate–sodium dodecyl sulphate (ZHN–SDS) nanocomposites, the molecular layer of SDS can be taken as the positively charged guest layer of LDH in order to balance the charge of the layer [16]. Therefore, it would be easiest for the pesticides to be intercalated into the interlayer of LHSs or LDHs especially for poor water-soluble pesticides.

Pesticides application are referred to the practical ways in which the pesticides are delivered to their biological target to make its more efficient and minimise their release into the environment and human exposure [17]. The main function of the pesticide application is to manages and control the use of pesticides that may lead to air pollution, water contamination and thus cause contaminated food. The World Health Organisation, 2019 reported that contaminated food causes more than 200 disease and that an estimated 600 million, about 1/10 of the humans in this world get sick due to contaminated food and about 420,000 die every year. This is because of contaminated food with harmful microorganism or chemical substances [18]. Chemical pesticides have greater chances to increase crop yield by controlling pests and disease in agriculture especially for all living things [19]. To increase crop production, pest management must be effective.

Fluazinam (FZ) which is also known by the IUPAC name of 3-chloro-*N*-(3-chloro-2,6-dinitro-4-trifluoromethylphenyl)-5-trifluoromethyl-2-pyridinamine with the chemical formula $C_{13}H_4Cl_2F_6N_4O_4$, is one of the few fungicides which is one of the group of pesticides that is unrelated to the dicarboximides and possesses a high level of activity against *sclerotinia blight* that resulted in excellent control in fields trials [20]. The structure of FZ is shown in Fig. 1. It exists as yellow crystals and it easily soluble in methanol, dichloromethane, acetone and the other organic solvents, however, it has poor solubility in water and alcohol [21].

One of the unique properties owned by FZ is as a protective fungicide that enables it to disturb the fungal cell process by uncoupling activity [22]. This material is also a broad spectrum fungicide which is widely used in agriculture against diseases such as potato blight [23]. Resistance of fungi to fungicides is a major problems to control the agricultural activity to fight plant pathogens [24]. Besides, this fungicide has a good residual effect and rain fastness even though it is a prophylactic fungicide [25].

Therefore, it is possible to intercalated the fungicides between the zinc hydroxide nitrate (ZHN) and sodium dodecyl sulphate (SDS) to balance the charged between ZHN for the agricultural sector.

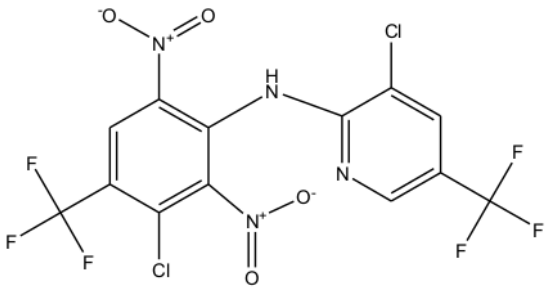

Fig. 1 The chemical structure of fluazinam

In this research, FZ was chosen to be inserted into the interlayer space of ZHN with the exist of sodium dodecyl sulphate (SDS) anion. To our knowledge, no study has yet been reported yet about the intercalation of FZ into the interlayer space of zinc hydroxide nitrate (ZHN) and sodium dodecyl sulphate (SDS) using an ion exchange reaction method. The controlled release of FZ from the ZHN–SDS–FZ nano host was studied in three release medium which were phosphate, carbonate and chloride solutions, and their release behaviour was observed and studied. The FZ fungicides used in the research will affect the fungus that causes the diseases in agriculture such as potato plantation. The fungicides will work by damaging the cell membrane of the fungus, inhibiting an important process in the fungus. The product can be formed as a tablet and a powder to be used on agricultural application.

2 Materials and methods

Zinc nitrate ($Zn(NO_3)_2{\cdot}6H_2O$) was purchased from System Malaysia, SDS from Across Organic and Sodium hydroxide (NaOH) from Sigma Aldrich. Meanwhile fluazinam fungicides, $C_{13}H_4Cl_2F_6N_4O_4$ (FZ) was purchased from Fisher Scientific. All chemicals were used without any further purification.

2.1 Synthesis of ZHN–SDS–FZ

The ZHN–SDS–FZ nano host was synthesised in a two-step process which were the co-precipitation method and the direct reaction methods. First, the co-preparation method was used to synthesise zinc hydroxide nitrate–sodium dodecyl sulphate (ZHN–SDS) by following a procedure described elsewhere [8]. Firstly, NaOH (1.0 M) and $Zn(NO_3)_2{\cdot}6H_2O$ at 40 mL were poured into 40 mL SDS (0.25 M) slowly. The pH value of the solution was adjusted until it reached 6.5.

Then, the obtained slurry mixture was aged at 70 °C for one day in an oil bath shaker. Then, the slurry was centrifuged at 4000 rpm for about 300 s to collect the precipitate and this was dried the at 60 °C in an oven. After that, the precipitation was ground into fine powder using a mortar, then stored in a sample bottle and labelled as ZHN–SDS.

In the second step, FZ was dissolved in dichloromethane (DCM) was prepared to be intercalated and added to the certain concentration of ZHN–SDS using an ion exchange method. The FZ solution (50 mL of 0.0125 M FZ solution) was poured into 0.3 g of synthesised ZHN–SDS to be dissociated in it. 50 mL of deionized water was added into the mixture and stirred for 2½ h. The slurry was aged at 70 °C for a day in an oil bath shaker. Then, the slurry was centrifuged at 4000 rpm for 300 s and the yellow precipitation was dried in an oven at 60° C for a day. Then, the precipitation was ground into a fine powder and kept in a sample bottle for characterisation purposes. Similar step was repeated using different concentration of FZ solution (0.025 M and 0.05 M).

2.2 Characterisation

The characterisation of the ZHN–SDS–FZ nano host was investigated by Powder X-Ray diffraction (PXRD), thermal analysis, Fourier transform infrared spectroscopy (FTIR), BET surface area, surface morphology analysis and elemental analysis. The PXRD was used over a scanning range of 2θ at 2°–60° with a scanning rate of 2° min^{-1} (30 kV and 15 mA). FTIR were recorded over the range 400–4000 cm^{-1} on a Perkin-Elmer spectrophotometer using the KBr disc method. Thermal analysis (TGA/DTG) was carried out using a Mettler Toledo TGA/SDTA851 analyser with a heating rate 10 °C min^{-1} between 35 and 1000 °C, under a nitrogen flow rate of about 50 ml min^{-1}. A CHNO-S analyser, model CHNS-O-932 of LECO Instruments was used for CHNO-S analyses. Then the elemental analysis of the nano host was determined by an inductively coupled plasma atomic emission spectrometry (ICP-OES) with a Perk-Elmer spectrophotometer model Optima 2000 DV. The BET surface area of the samples was determined using nitrogen gas adsorption–desorption technique at 77 K together with the BET equation. The surface morphology of ZHN–SDS–FZ was observed using high-resolution field emission scanning electron microscope (FESEM) (Hitachi SU 8020 UHR, Japan).

2.3 Controlled release study of nano host

The controlled release study of ZHN–SDS–FZ using phosphate solution (Na_3PO_4), carbonate solution (Na_2CO_3), and chloride solution (NaCl) as a model was performed with three concentrations which were 0.3, 0.5, and 1.0 M using a UV–visible spectrophotometer. 0.6 mg was dispersed in the solution for the ion exchange process as reported in the previous study [26] in order to study the release of FZ from ZHN–SDS by the selected solution [12]. The amount of FZ released from the interlayer space of ZHN–SDS–FZ into the solution was recorded at the present time with $\lambda_{max} = 245.5$ nm.

3 Results and discussion

3.1 Powder X-ray diffraction (PXRD) analysis

PXRD analysis is one of the characterisation techniques used to prove that the intercalation of FZ into ZHN–SDS has successfully achieved, and the PXRD pattern for FZ, ZHN–SDS and the resulting ZHN–SDS–FZ nano host are shown in Fig. 2. The intercalation of a surfactant which is SDS enables the enlargement of the size of ZHN effectively delaminating it [27], thus making it easier for FZ to be intercalated. SDS carries negative charges which

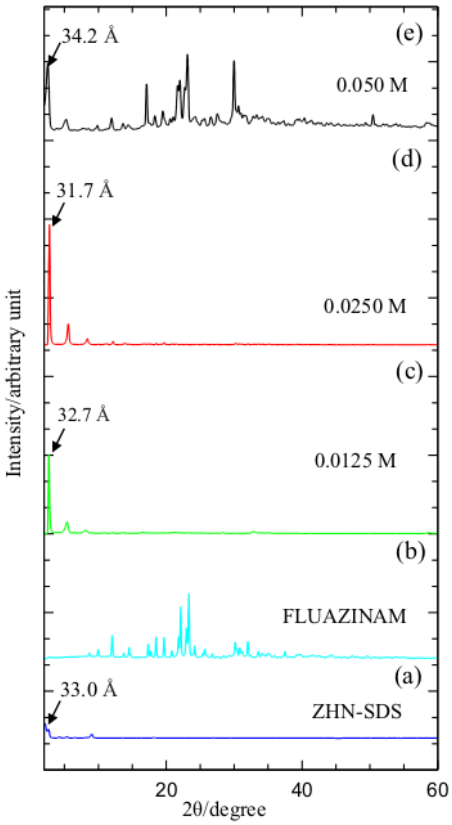

Fig. 2 PXRD pattern of ZHN–SDS (**a**) and the ZHN–SDS–FZ nano host with various concentration of FLUAZINAM (FZ) (**b**) 0.0125 M (**c**), 0.0250 M (**d**) and 0.050 M (**e**) (Color figure online)

allow the establishment of electrostatic interactions with the ZHN interlayer during the intercalation of SDS [28]. This is due to the SDS containing three oxygen atoms (SO_3 group). The basal spacing of ZHN–SDS at 33.0 Å reveals that the SDS were located perpendicular to become a monolayer arrangement in the interlayer space of ZHN. As the FZ is inserted, the negative charge of FZ is attracted to the positive charge between the interlayer of ZHN. Both SDS and FZ stays in their position in the interlayer space of ZHN due to an electrostatic interaction. Moreover, the PXRD diffraction patterns of the ZHN–SDS–FZ nano host are characteristic of a structural disorganisation, exhibiting a turbostatic effect denoted by the enlargement of the interlayer space of the nano host and the weak bond interactions between the interlayer of the host and the guest anions [29]. Meanwhile, the crystallinity of ZHN–SDS–FZ nano host is lower than that for the ZHN–SDS which located at 33.0 Å due to steric hindrance by water molecules coordinated to the zinc tetrahedrons [30]. The decreasing of intensity peak at lower 2θ for (c), (d) and (e) compared to the (a) XRD pattern that same as reported as the intensity peaks for TBD-LDH catalysts decreased as compared to SDS-LDH structures as the SDS are exchanged with TBD moieties [31].

By subtracting the hydroxide plate thickness which is 4.8 Å [32], which the inorganic layers formed by Zn^{2+} cations as same as LDH [13], and each tetrahedrons (2.6 Å X 2) make the interlayer space that available for the SDS and FZ was calculated to be 21.7 Å. Therefore, it is acceptable to subtract 4.8 Å of Zn^{2+} and each tetrahedron to determine the space in the interlayer space of ZHN as shown in Fig. 5. The ZHN–SDS–FZ diffraction peak in Fig. 2 shows that the nano host presented an expanded basal spacing of 31.7 Å for 0.025 M of FZ anion. Considering that FZ are inserted into the interlayer space of ZHN–SDS–FZ nano host through electrostatic attractions and hydrogen bonds to water molecules located at the zinc tetrahedral apex, the proposed nano host by intercalation and the value of the basal spacing are illustrated in Fig. 5. The intercalated peak at 2θ of the nano host shows a slight decrease of basal spacing as the FZ concentration increases. This is because of the adsorption at different orientation angles in the interlayer of the nano host [33].

As a result, ZHN–SDS–FZ nano host prepared using 0.025 M as a complete ion exchange produced sharp peaks compared to 0.0125 M and 0.50 M. The ZHN–SDS–FZ diffraction peak in Fig. 2 proves that the nano host was successfully synthesised. This complete synthesised of the nano host was chosen as a well-ordered nano host to be used in the next characterisation.

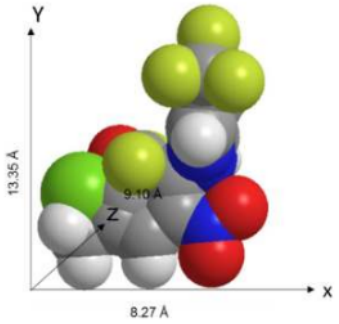

Fig. 4 3-D molecular structure of the FZ

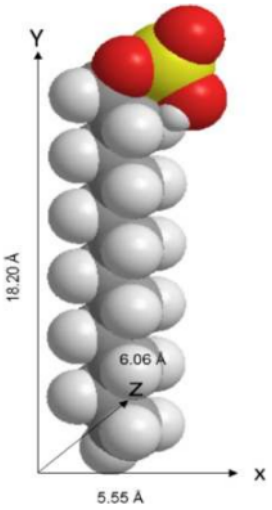

Fig. 3 3-D molecular structure of the SDS

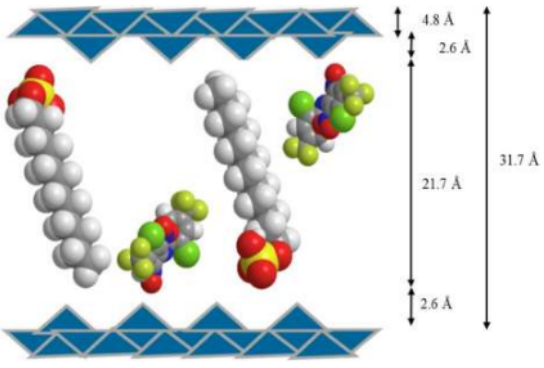

Fig. 5 The proposed spatial orientation of FZ in the interlayer space of ZHN–SDS–FZ nano host

3.2 Spatial orientation of ZHN–SDS–FZ nano host

Chem 3D Ultra software was used to propose an orientation of SDS (Fig. 3), FZ (Fig. 4) and ZHN–SDS–FZ nano host (Fig. 5). The x, y and z axes of FZ were determined to be 8.2 Å,13.3 Å and 9.1 Å respectively, whereas the x, y and z axes of SDS were determined to be 5.5 Å, 18.2 Å, and 6.0 Å respectively. The schemed spatial orientation of FZ in the ZHN–SDS interlayer space is obtained based on the basal spacing observed from PXRD analysis. The negatively charged FZ is arranged parallel to surfactant SDS in monolayer arrangement, where the negative charge of FZ is attracted to the positively charged ZHN layer via electrostatic force. The basal spacing in PXRD of ZHN–SDS- FZ is 31.7 Å and the interlayer height of the nano host is determined to be about 21.7 Å, which was obtained by subtracting the thickness of ZHN layer at 4.8 Å, and the thickness of the Zn tetrahedron at 2.6 Å/each. For the SDS molecules, it was believed they stay in the monolayer arrangement because the values are very close between SDS and the interlayer height of the nano host where the values are 18.2 Å and 21.7 Å respectively [34]. This is due to the axis of the SDS molecule being 18.2 Å which it was the longest axis as shown in Fig. 3. The proposed orientation of the SDS and FZ in the interlayer of ZHN were predicted and illustrated in Fig. 5.

3.3 Fourier transform infrared (FTIR) analysis

The successful FZ intercalated into the interlayer space of ZHN–SDS were supported by FTIR analysis. ZHN–SDS, FZ and the ZHN–SDS–FZ nano host spectra are shown in Fig. 6.

The FTIR spectra of 3570 cm^{-1} shows a strong and sharp band due to the OH group of the free H_2O molecule of ZHN–SDS–FZ (O–H stretch). Whereas at 3461 cm^{-1} it shows the strong and broad absorption (OH vibration). This is because of the hydrogen bond that is formed between the H_2O molecule. The band at 1637 cm^{-1} is referred to the H_2O that is present in the ZHN–SDS layer. There are two main doublet absorption bands existing at 2846 cm^{-1} and 2913 cm^{-1} which are referred to an aliphatic group (stretching vibration), while, the band at 1458 cm^{-1} refers to the aliphatic group (bending vibration). For SDS molecules, bands can be seen at 1220 cm^{-1} and 1084 cm^{-1} that show it is a sulphate group (S=O). While the presence of nitrate ion (NO_3) at 1364 cm^{-1} show a strong absorption band affirming that the zinc nitrate was used as the metal ion which contributed to zinc hydroxide nitrate (ZHN).

Also shown in Fig. 6, ZHN–SDS–FZ displays several peaks that existence the peak of FZ and ZHN–SDS. For the hydroxyl group of the water molecule, a strong and broad band displays at 3498 cm^{-1}, while a band at 1602 cm^{-1} shows that there are free water molecules in the interlayer

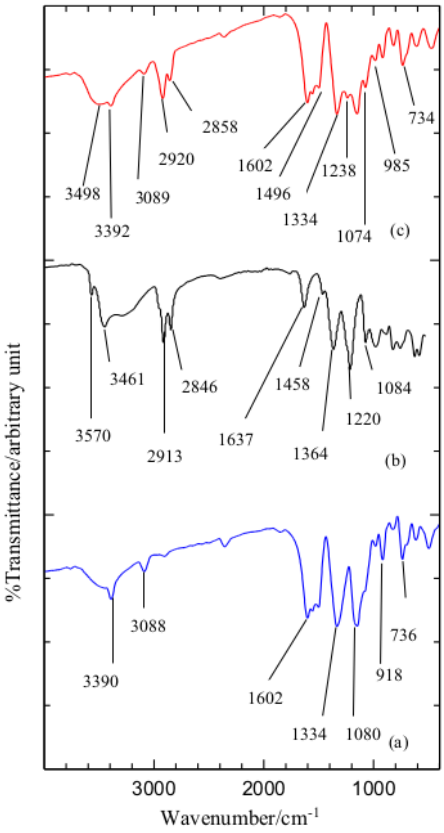

Fig. 6 FTIR spectra of **a** FZ, **b** ZHN–SDS, **c** ZHN–SDS–FZ nano host

space of the ZHN–SDS–FZ nano host. A sharp doublet absorption of the ZHN–SDS–FZ nano hosts resembles the band in ZHN–SDS layer at 2858 and 2920 cm^{-1} refer to the (C–H stretch) group that is present in the nano hosts. The bands appearing at 1238 and 1074 cm^{-1} are assigned to the sulphate group S=O (asymmetric and symmetric stretching vibration). This shows that SDS molecules exist in the both interlayer space of ZHN–SDS and the ZHN–SDS–FZ nano host.

The typical absorption band of FZ that appear in ZHN–SDS–FZ nano host spectra at 1334 cm^{-1}, 985 cm^{-1} and 734 cm^{-1} are due to the stretching vibration of C–F, C–N and C–Cl respectively. Two strong bands of N–O stretching in the FZ spectra at 1500 cm^{-1} and 1558 cm^{-1} also appear in the ZHN–SDS–FZ at 1496 cm^{-1} and 1558 cm^{-1}. The N–O band at 1364 cm^{-1} in the ZHN–SDS spectra disappeared in the ZHN–SDS–FZ spectra, which affirms that NO^{3} has been removed after the ion exchange process for FZ to be intercalated into the interlayer of

ZHN. Moreover, the bands of N–H stretching for aliphatic amine at 3390 cm^{-1} in FZ spectra appeared in the ZHN–SDS–FZ spectra at 3392 cm^{-1}. The medium weak band of C=C aromatic at 1602 cm^{-1} also appeared in the ZHN–SDS–FZ spectra indicating that FZ has been successfully intercalated into the ZHN–SDS interlayer space. However, the position of these bands was slightly different because of a slightly shifted due to an interaction between FZ, SDS and ZHN to form ZHN–SDS–FZ nano host. This was due to the FZ and H_2O in the interlayer space being free to move by breaking bonds to the layer and forming new ones [35]. In general, H_2O is held through the formation of hydrogen bond with the hydroxide layer and/or with the interlayer anion [36]. The bands that appeared in the FTIR spectra that were assigned to FZ, ZHN–SDS, and the ZHN–SDS–FZ nano host are summarised in Table 1.

Table 1 FTIR bands for ZHN–SDS, fluazinam anion and ZHN–SDS–FZ nano host

Characteristic group	ZHN–SDS (cm^{-1})	ZHN–SDS–FZ (cm^{-1})	Fluazinam (cm^{-1})
(O–H), H-bonded	3461	–	–
(O–H), H_2O	3570	3498	–
(N–H) stretch	–	3392	3390
(=C–H) stretch	–	3089	3088
(H–O–H), H_2O in the layer	1637	–	–
(C–Cl)	–	734	736
(C–F)	–	1334	1334
(C–N)	–	985	1080
(C–H) stretching	2846	2858	–
	2913	2920	–
(C–H) bending	1458	–	–
(N–O) stretching	–	1496	1500
	–	1558	1558
(S=O)	1220	1238	–
	1084	1074	–
C=C aromatic medium weak	–	1602	1602

3.4 Elemental analysis

The TGA/DTG analysis of ZHN–SDS and ZHN–SDS–FZ nano host are shown in Table 2. It shows that ZHN–SDS contains 24.8% carbon, 5.5% hydrogen, 2.5% nitrogen and 3.4% sulphur, while the ZHN–SDS–FZ nano host contains 31.4% carbon, 1.2% hydrogen, 7.9% nitrogen, and 3.1% sulphur. The percentage loading of FZ in the interlayer of ZHN–SDS was calculated to be 65.6%. The existence of the FZ anion in the nano host was proven which supports the successful intercalation of FZ into its nano host. Therefore, the nitrogen for ZHN–SDS–FZ nano host was contributed by the FZ anion.

The percentages of Zn in the ZHN–SDS–FZ nano host was determined to be 11.5% from ICP-OES analysis. Data obtained for the peak of NO_3^- in the interlayer space of ZHN no longer exists in the nano host spectra which contributed to ZHN–SDS–FZ nano host. This means that all the NO_3^- have been replaced by FZ anions due to ion exchange methods during the intercalation process as shown in the PXRD and FTIR analysis. The proposed chemical formula for ZHN–SDS–FZ nano host formed from the elemental analysis is $Zn(OH)_{0.18}(CH_3(CH_2)_{11}SO_4)_{0.10}(C_{13}H_4Cl_2F_6N_4O_4)_{0.14}{\cdot}1.54H_2O$.

3.5 Thermal analysis (TGA/DTG)

Figure 7 shows the thermal decomposition behaviour for FZ, ZHN–SDS–FZ nano host and ZHN–SDS. In Fig. 7a, 2 stages of decomposition of FZ were observed, the first decomposition at 217 °C with a 35.2% weight loss, and a second decomposition at 301 °C with the weight loss of 62.2%. This shows that the optimum temperature of FZ occurred.

For ZHN–SDS–FZ nano host, four steps of decomposition observed as shown in Fig. 7c. The first step of thermal decomposition with minor weight loss of 13.6% at 186 °C is related to an elimination of water molecules that exist in the interlayer space of ZHN–SDS. The second step of thermal decomposition at 216 °C with a weight loss of 20.4% refers to the decomposition of SDS. While the third step of thermal

Table 2 Elemental analysis composition of ZHN–SDS and ZHN–SDS–FZ nano host

Sample	C (%)	H (%)	N (%)	S (%)	FZ (% w/w)[a]	Formula[b]
ZHN–SDS	24.8	5.5	2.5	3.4	–	–
ZHN–SDS–FZ	31.4	1.2	7.9	3.1	65.6%	$Zn(OH)_{0.18}(CH_3(CH_2)_{11}SO_4)_{0.10}(C_{13}H_4Cl_2F_6N_4O_4)_{0.14}{\cdot}1.54H_2O$

[a]Estimated from CHNS analysis

[b]Estimated from ICP/OES, CHNS and TGA/DTG analysis

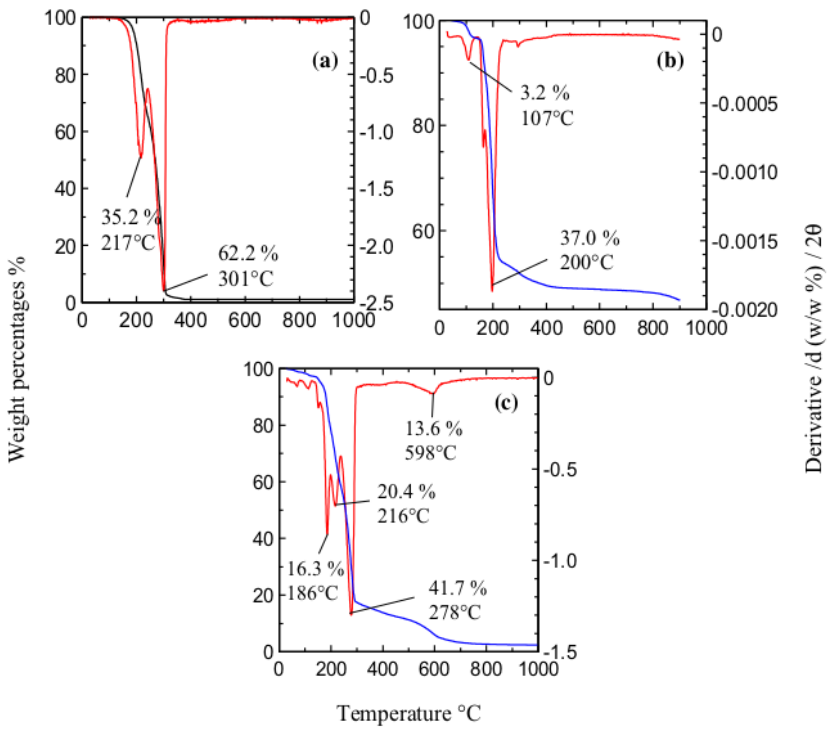

Fig. 7 Thermogravimetric analysis (TGA/DTG) of **a** FZ **b** ZHN–SDS **c** ZHN–SDS–FZ nano host (Color figure online)

decomposition corresponding to the decomposition of FZ which it was decomposed at 278 °C with a 41.7% weight loss. The last step of thermal decomposition with a 16.3% weight loss at 598 °C is the complete decomposition of the ZHN–SDS–FZ nano host.

From Fig. 7b, it can be seen that the ZHN–SDS display two steps of weight loss. The first step is due to the escape of physiosorbed water at 107 °C with a 3.2% of weight loss in the interlayer space. Whereas at 200 °C and with a 37.0% weight loss, the decomposition of SDS occurred. The optimum temperature of the decomposition of FZ in the ZHN–SDS–FZ nano host increased from 301 °C to 598 °C as shown in Fig. 7a, c. Therefore, the thermal stability of ZHN–SDS–FZ nano host prove that the FZ which is intercalated in the ZHN–SDS interlayer space is stable compared to the pure FZ.

3.6 Surface morphology analysis

From Fig. 8 it can be seen that there is obviously a different surface morphology of ZHN–SDS and ZHN–SDS–FZ nano host. ZHN–SDS shows a flake-like structure with a rough surface [37], while the ZHN–SDS–FZ nano host shows a thin lamellar flake-like sheet structure which seen obviously changes on their surface that inclined to the formation of a flaking and wrinkly layer that make the agglomerates structure of ZHN–SDS. The changes of surface morphology between Fig. 8a, b prove that FZ was successfully intercalated into the interlayer of ZHN–SDS.

3.7 Surface area analysis

The surface area analysis of ZHN–SDS and ZHN–SDS–FZ nano host were also characterised. The surface area of ZHN–SDS and ZHN–SDS–FZ nano host shown in Table 3 were calculated by Brunauer–Emmett–Teller (BET) method.

Table 3 and Fig. 9 show the surface area, pore diameter and the classification of porosity between ZHN–SDS and ZHN–SDS–FZ nano-host. The surface area of ZHN–SDS is 2.03 m^2/g. After the intercalation, the value was increased to 2.07 m^2/g. The increased surface area of ZHN–SDS–FZ nano host causes a pore size decrease while the pore volume was increased. Figure 9a ZHN–SDS show a mesoporous material with Type IV isotherm [37], while the resulting nano host shows a macro porous material with Type III isotherm that studied by multilayer at high relative pressure [38]. The curve increase when the lateral interaction between the absorbate molecules is stronger than the interaction between the adsorbate and the adsorbent surface [39], which is the driving force of the adsorption process, resulting in an accelerated uptake at higher relative pressure [40]. Based on Fig. 9a, a very low uptake until $P/P_o > 0.8$ indicated a poor

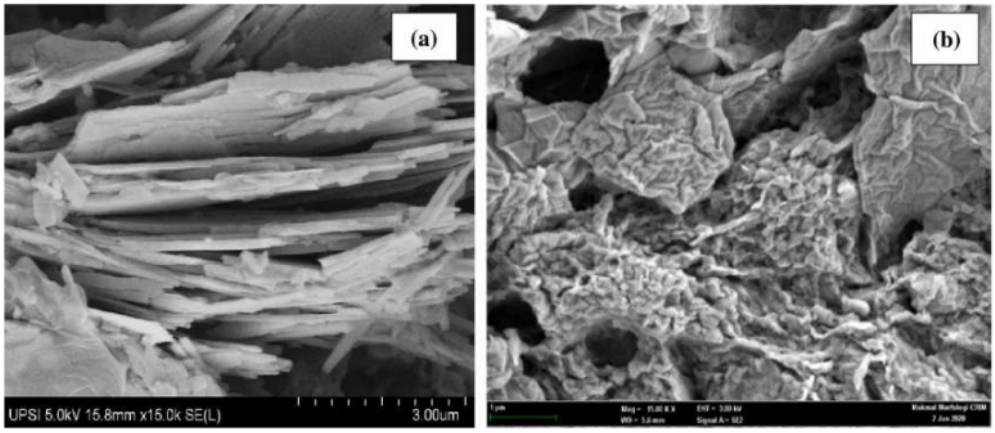

Fig. 8 FESEM micrograph of ZHN–SDS **a** and ZHN–SDS–FZ **b** at 15 K magnification nano host

Table 3 Surface properties of ZHN–SDS and ZHN–SDS–FZ nano host

Samples	Surface area (m^2/g)	Pore diameter (Å)	Classification
ZHN–SDS	2.03	133.59	Mesoporous
ZHN–SDS–FZ	2.07	111.89	macroporous

interaction between the adsorbate-adsorbent, while Fig. 9b shows P/P_o exceeded 0.8 which means that the amount of adsorbed gas is increasing exponentially, due to the stronger interaction between the adsorbate-adsorbent. Even though, the specific BET surface area of ZHN–SDS–FZ nano host are higher than ZHN–SDS, the average pore diameter (Å) of ZHN–SDS–FZ is lower compared to the ZHN–SDS revealing that FZ is more porous than ZHN–SDS.[41].

Figure 10 shows the Barrett-Joyner-Halenda (BJH) desorption pore size distributions (PSD) for ZHN–SDS and ZHN–SDS–FZ nano host. BJH average pore diameters were determined to be 37.5 nm and 35.5 nm for ZHN–SDS and ZHN–SDS–FZ nano host respectively. This is because of the changes of the pore size distribution after the intercalation process by FZ, makes the FZ is selectively formed in the ZHN–SDS layer [42]. The modification of the pores happened because the initial slope of Types III was zero at low relative pressure. This does not allow for an estimation of the solids monolayer surface compared to the adsorbate–adsorbate interaction [43]. This is because of the smaller size of particle will fill the larger unoccupied spaces among the larger particles that may lead to the existence of larger pore sizes. Therefore, the porosity of the ZHN–SDS–FZ nano host is macroporous.

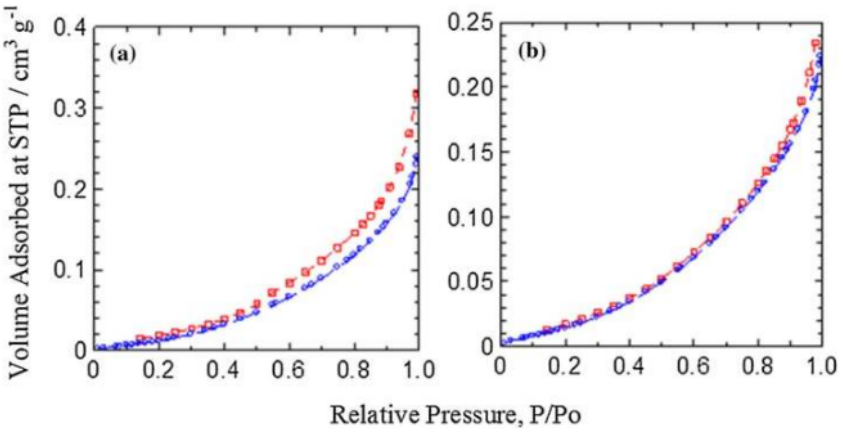

Fig. 9 Surface area for **a** ZHN–SDS and **b** ZHN–SDS–FZ nano host

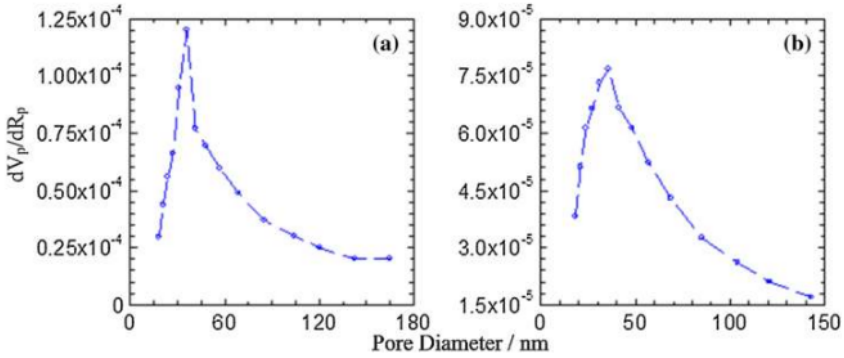

Fig. 10 BJH desorption pore size distributions for **a** ZHN–SDS and **b** ZHN–SDS–FZ nano host

3.8 Controlled release of ZHN–SDS–FZ nano host

The controlled release study of ZHN–SDS–FZ nano host was studied by using three different concentrations of phosphate solution (Na_3PO_4), carbonate solution (Na_2CO_3) and chloride solution (NaCl). Phosphate ions, carbonate ions and chloride ions were chosen as release medium because these solution are present in the soil composition and in the rain water [44]. The intercalated FZ in the interlayer of ZHN–SDS can be released and undergo an ion exchanged process with anions in the release medium [45].

This release profiles in Fig. 11 give significant information on the percentage releases that were investigated when the type and concentration of the solutions were used in this controlled release of ZHN–SDS–FZ nano host. Figure 11a shows that at 0.3 M, 0.5 M and 1.0 M of phosphate solution, the accumulated percentages release was 49.4%, 87.3% and 92.4% respectively. The accumulated percentage release of FZ from the interlayer space of the ZHN–SDS–FZ nano host increases as the concentration increased. This observation of the release according to their time for FZ release in 0.3 M, 0.5 M and 1.0 M of phosphate solution was achieved in 1598 min, 1386 min and 1200 min respectively. The early fast release is possibly attributed to the release of FZ from the nano host. Then the slow release is due to the exchange of anion in the internal part with anions in ZHN–SDS interlayer. The time taken for release the FZ anion from ZHN–SDS matrices is longer because they have a strong host–guest interaction [46].

In Fig. 11b, the accumulated percentage of FZ release from the interlayer space of ZHN–SDS–FZ nano host in the carbonate solution at three concentrations of 0.3 M, 0.5 M and 1.0 M were 52.4%, 85.6% and 92.7% respectively. The times taken for the FZ to be release in the carbonate solution were 3975 min, 3862 min, and 3740 min, respectively, which is longer compared to the release of FZ in the phosphate solutions. The times taken increases up to 4000 min until the release process reaches the higher percentage of release and achieves equilibrium. The release rate of carbonate solution was the slowest release of FZ compared to the phosphate solution.

Figure 11c shows that the release of ZHN–SDS–FZ nano host in the chloride solution allowed the released of 46.1% (7883 min) at 0.3 M, 56.4% (7808 min) at 0.5 M, and 61.7% (7752 min) at 1.0 M of carbonate solution, and all the concentrations reached equilibrium at 8000 min determined by

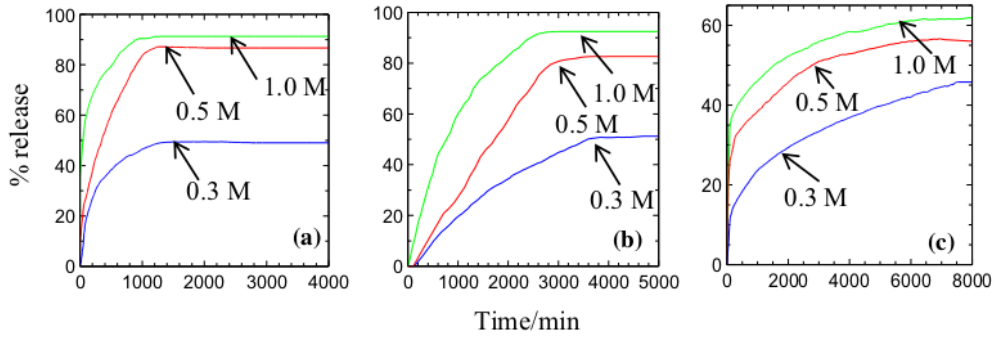

Fig. 11 Release profile of FZ from ZHN–SDS–FZ nano host into 3 different concentration which are 0.1, 0.5 and 1.0 M concentration of **a** Phosphate (Na_3PO_4) **b** Carbonate (Na_2CO_4) and **c** Chloride (NaCl) solution (Color figure online)

all the FZ anions having been released from the interlayer ZHN–SDS–FZ nano host. The accumulated percentages of FZ released from ZHN–SDS–FZ nano host increases in the order of 0.3 M < 0.5 M < 1.0 M. As the concentration increases, the times taken for FZ to be released from ZHN–SDS–FZ nano host in chloride solution decreases due to the release medium being monovalent ions that are more difficult to undergo an ion exchange process because the chloride ions (Cl^-) have a lower charge density, therefore the times for the slowest release process happened. Therefore, the release rate of chloride solution was the slowest release of FZ compared to the phosphate and carbonate solutions.

In the release medium, affinity is related with the release rate of the FZ from ZHN–SDS interlayer. The percentage of accumulated percentages release of FZ in the aqueous solution is in the order of PO_4^{3-} and $CO_3^{2-} > Cl^-$. This is due to the PO_4^{3-} and CO_3^{2-} having higher affinity compared to the Cl^- which has lower affinity due to it is monovalent ion. It shows that the affinity is important for controlled release study of ZHN–SDS–FZ nano host. The presence of PO_4^{3-}, CO_3^{2-} and Cl^- attributed to an ion exchange affinity towards ZHN–SDS interlayer, can determines the amount of FZ to be released.

Based on the release profile, the result showed the affinity of anion plays an important rule for controlled release from the interlayer ZHN–SDS–FZ nano host. The ion exchange of incoming anions increases with increasing charge density and decreasing ionic radius proven that phosphate and carbonate solution has higher affinity compare to the chloride solution. It also shown that aqueous solutions involving phosphate and carbonate solution have a higher percentage of accumulated released of FZ compared to the chloride solution. This is due to phosphate and carbonate having a higher affinity towards the ZHN–SDS interlayer. It was proven that both of phosphate and carbonate solution give excellent release process compared to chloride solutions. The presence chloride solution give significantly that encourages the release process of FZ decelerate release process and lower the percentages accumulated release. Therefore, chloride solution can act as a release medium which has the slowest release process, which means the release rate is slowest compared to phosphate solutions that have a faster released from the interlayer.

3.9 Kinetic study

There are five kinetic model of FZ releases from the interlayer of ZHN–SDS–FZ nano host to further clarify the mechanism by which to understand the FZ release from the nano host. The five different kinetic models from commonly used in this research for the kinetics study are the zeroth order (Eq. 1) [47], first order (Eq. 2) [48], pseudo-second order (Eq. 3) [49], parabolic diffusion (Eq. 4) and fickian diffusion (Eq. 5) [50].

The parameter correlation coefficient (r^2) and $t_{1/2}$ values are determined by calculation based on the equation below, and $t_{1/2}$ values means the time taken of 50% for release of the FZ anions from the interlayer ZHN–SDS–FZ nano host which were calculated manually from the graph.

$$\text{Zeroth order } x = t + c \tag{1}$$

$$\text{First order} - \log\left(1 - M_i/M_f\right) = t + c \tag{2}$$

$$\text{Pseudo-second order } t/M_i = 1/\left(M_f^2\right) + t/M_f \tag{3}$$

$$\text{Parabolic diffusion } M_i/M_f = kt^{0.5} + c \tag{4}$$

$$\text{Fickian diffusion } M_i/M_f = kt^n \tag{5}$$

Figures 12, 13, and 14 shows the fitted release data of ZHN–SDS–FZ nano host into three different release mediums into the five kinetic models. Based on the data obtained, ZHN–SDS–FZ nano host followed the pseudo-second order with a good fit for phosphate, carbonate and chloride solutions, with a maximum coefficient nearest to 1.00 which it is the best fit of the FZ release profiles. Furthermore, it confirms that a pseudo second order model was involved in the dissolution of ZHN–SDS–FZ nano host due to the swelling of the structure, as well as the FZ anion between ZHN–SDS with the NO_3^- that is present at the ZHN–SDS layer in the aqueous solution [51].

Based on data obtained for all the concentration as shown in Table 4, the time taken for 50% FZ to be released or we called it as half-life $t_{1/2}$ was decreased due to the high accumulated percentages in all release medium which were 92.4%, 92.7% and 61.7% of 1.0 M in the phosphate, carbonate and chloride solutions respectively. The $t_{1/2}$ for low accumulated percentages of 0.3 M of release medium was increased due to the fact that more ions can be replaced in the interlayer of FZ making the release rate the fastest compared to the other concentrations by the ion exchange process. As the release process of FZ anion using release medium which are phosphate, carbonate and chloride solution, it can be seen that the pseudo second order model is better fitted that the other kinetic model ($0.900 < r^2 < 1.000$). Therefore, the release mechanism happened by pseudo order model via dissolution of the ZHN–SDS–FZ nano host and the ion exchange between the intercalated FZ and the release medium [51].

4 Conclusion

ZHN–SDS–FZ nano host was synthesised using ion exchange method in the presence of SDS surfactant to enlarge the layer of ZHN for the FZ to be intercalated. The intercalation was successful with a basal spacing of 31.7 Å

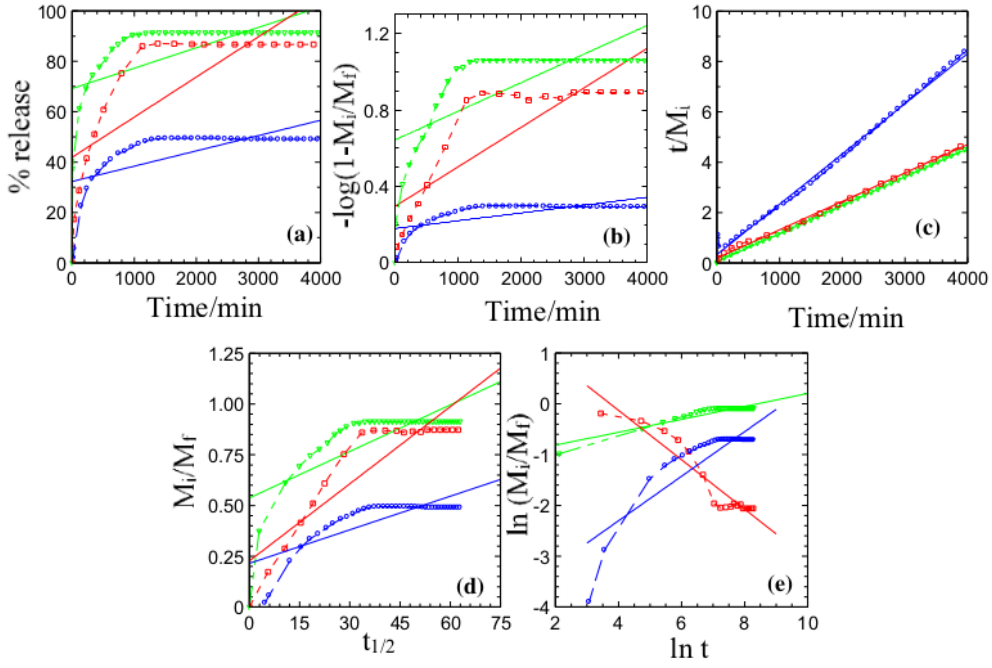

Fig. 12 Fitting data of the FZ release data into 0.3 (blue), 0.5 (red) and 1.0 (green) M concentration of phosphate solution to the **a** zeroth order model, **b** first order model, **c** pseudo- second order model, **d** parabolic diffusion model and **e** fickian diffusion model (Color figure online)

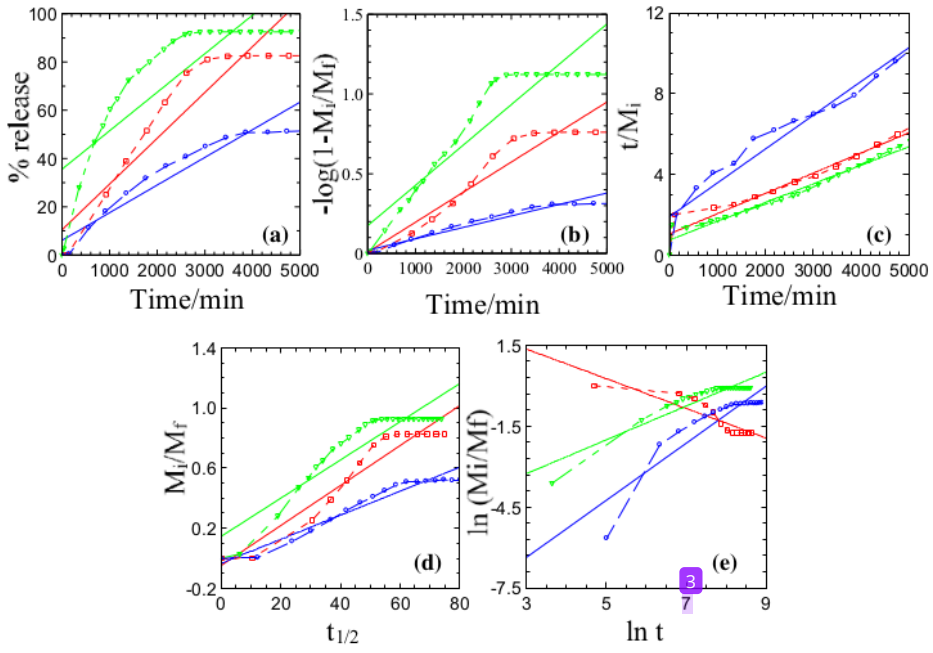

Fig. 13 Fitting data of the FZ release data into 0.3 (blue), 0.5 (red) and 1.0 (green) M concentration of carbonate at the **a** zeroth order model, **b** first order model, **c** pseudo- second order model, **d** parabolic diffusion model and **e** fickian diffusion model (Color figure online)

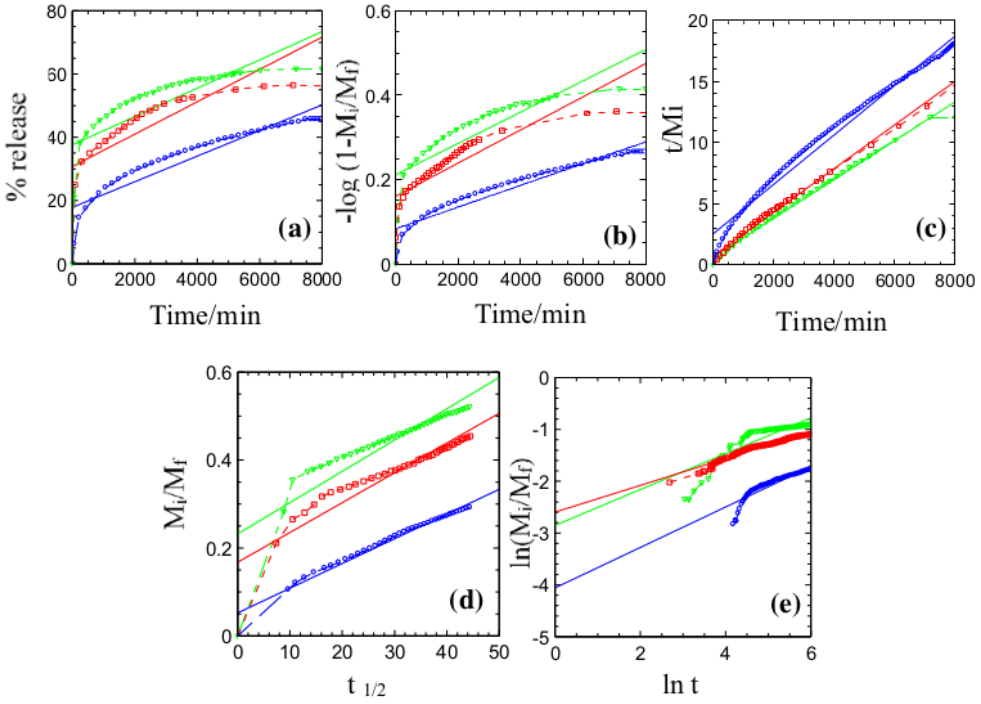

Fig. 14 Fitting data of the FZ release data into 0.3 (blue), 0.5 (red) and 1.0 (green) M concentration of chloride solution to the **a** zeroth order model, **b** first order model, **c** pseudo- second order model, **d** parabolic diffusion model and **e** fickian diffusion model (Color figure online)

Table 4 Correlation coefficients (r^2) and half-life ($t_{1/2}$) obtained from the data of FZ release from the interlayers of ZHN–SDS–FZ nano host into phosphate, carbonate and chloride solution

Concentration (M)	Zeroth order model	First order model	Parabolic diffusion model	Fickian diffusion model	Pseudo-second order model	
	r^2					$t_{1/2}$ (min)
Phosphate solution (Na_2PO_4)						
0.3	0.424	0.471	0.636	0.752	0.996	133.19
0.5	0.595	0.703	0.814	0.905	0.997	40.45
1.0	0.314	0.490	0.542	0.861	1.00	33.29
Carbonate solution (Na_2CO_3)						
0.3	0.923	0.959	0.955	0.813	0.953	1373.57
0.5	0.882	0.932	0.928	0.800	0.932	1399.55
1.0	0.704	0.869	0.860	0.869	0.968	665.23
Chloride solution (NaCl)						
0.3	0.851	0.991	0.974	0.870	0.981	932.36
0.5	0.589	0.673	0.848	0.971	0.991	183.45
1.0	0.547	0.652	0.762	0.738	0.991	100.56

based on the PXRD result. The characterisation studies of FTIR, ICP-OES, and CHNS analyses also proved that the FZ has been successfully intercalated in the ZHN–SDS layer space. The percentage loading of nitrogen is estimated at 65.6% was supported due to the nitrogen that contributes to the FZ in the ZHN–SDS–FZ nano host. The thermal stability of FZ was also significant that was highlighted in the thermogravimetric analysis in which the ZHN–SDS–FZ nano host is thermally stable compared to the pure FZ. Moreover, there are changes in surface morphology analysis in

which the ZHN–SDS shows flake-like structure, while ZHN–SDS–FZ nano host shows a thin lamellar flake-like sheet structure. The controlled release of FZ has a higher percentage of release in phosphate and carbonate solutions at 92.4% and 92.7% respectively. All the release medium was followed a pseudo-second order model for the kinetic study of release of ZHN–SDS–FZ nano host. Therefore, ZHN can be proposed as an excellent host and a good material for the slow release of FZ for agricultural purposes.

Acknowledgements This research was supported by Ministry of Education (MOE) through Fundamental Research Grant Scheme (2019-0002-102-02) and would like to thanks UPSI for all funding and support for this research.

Compliance with ethical standards

Conflict of interest No potential conflict of interest was reported by the authors.

References

1. S.P. Newman, W. Jones, J. Solid State Chem. **148**, 26 (1999)
2. R.A. Schoonheydt, T. Pinnavaia, G. Lagaly, N. Gangas, Pure Appl. Chem. **71**, 2367 (2007)
3. T.H. Kim, I. Heo, S.M. Paek, C.B. Park, A.J. Choi, S.H. Lee, J.H. Choy, J.M. Oh, Bull. Korean Chem. Soc. **33**, 1845 (2012)
4. M. Ezoddin, L. Adlnasab, A. Afshari Kaveh, M. A. Karimi, B. Mahjoob, Biomed. Chromatogr. 1 (2019).
5. T. Biswick, D.H. Park, Y.G. Shul, J.H. Choy, J. Phys. Chem. Solids **71**, 647 (2010)
6. H. Nakayama, A. Hatakeyama, M. Tsuhako, Int. J. Pharm. **393**, 105 (2010)
7. N. Hashim, S.N.M. Sharif, Z. Muda, I.M. Isa, N.M. Ali, S.A. Bakar, S.M. Sidik, M.Z. Hussein, Mater. Res. Innov. **8917**, 1 (2018)
8. J. Liu, X. Zhang, Y. Zhang, ACS Appl. Mater. Interfaces. **7**, 11180 (2015)
9. C. Markland, G.R. Williams, D. O'Hare, J. Mater. Chem. **21**, 17896 (2011)
10. T. Kameda and T. Yoshioka, Intech 124 (2011).
11. M.Z. Hussein, N.F.B. Nazarudin, S.H. Sarijo, M.A. Yarmo, J. Nanomater. **2012**, 1 (2012)
12. A.F.A. Latip, M.Z. Hussein, J. Stanslas, C.C. Wong, R. Adnan, Chem. Central J. **7**, 1 (2013)
13. A.C.T. Cursino, V. Rives, G.G.C. Arizaga, R. Trujillano, F. Wypych, Mater. Res. Bull. **70**, 336 (2015)
14. N. Hashim, S.N.M. Sharif, I.M. Isa, S.A. Hamid, M.Z. Hussein, S.A. Bakar, M. Mamat, J. Phys. Chem. Solids **105**, 35 (2017)
15. I.F. Mustafa, M.Z. Hussein, B. Saifullah, A.S. Idris, N.H.Z. Hilmi, S. Fakurazi, J. Agric. Food Chem. **66**, 806 (2018)
16. S. Babakhani, Z.A. Talib, M.Z.B. Hussein, A.A.A. Ahmed, Adv. Mater. Res. **1024**, 52 (2014)
17. R. Bateman, Optim. Pestic. Use 131 (2004).
18. World Health Organization, Blackwell Publishing, pp. 1–62 (2019).
19. P. Nicolopoulou-Stamati, S. Maipas, C. Kotampasi, P. Stamatis, L. Hens, Front. Public Health **4**, 148 (2016)
20. F.D. Smith, P.M. Phipps, R.J. Stipes, Peanut Sci. **19**, 115 (2010)
21. A. Draper, P. Cullinan, C. Campbell, M. Jones, A.N. Taylor, Occup. Environ. Med. **60**, 76 (2003)
22. Z.J. Guo, H. Miyoshi, T. Komyoji, T. Haga, T. Fujita, Bioenergetics **1056**, 89 (1991)
23. H.T.A.M. Schepers, G.J.T. Kessel, F. Lucca, M.G. Förch, G.B.M. van den Bosch, C.G. Topper, A. Evenhuis, Eur. J. Plant Pathol. **151**, 947 (2018)
24. H. Ishii, Jpn. Agric. Res. Q. **40**, 205 (2006)
25. R.M. Niemi, I. Heiskanen, J.H. Ahtiainen, A. Rahkonen, K. Mäntykoski, L. Welling, P. Laitinen, P. Ruuttunen, Appl. Soil. Ecol. **41**, 293 (2009)
26. S.H.H.A. Ali, M. Al-Qubaisi, M.Z. Hussein, Z. Zainal, M.N. Hakim, Int. J. Nanomed. **6**, 3099 (2011)
27. Y. Zhang, H.Y. Sun, X. Bai, Y. Li, J. Zhang, M. Zhao, X. Huang, C.Y. Feng, Y. Zhao, J. Dispers. Sci. Technol. **40**, 811 (2019)
28. D. Kostadinova, A.C. Pereira, M. Lansalot, F. D'Agosto, E. Bourgeat-Lami, F. Leroux, C. Taviot-Guého, S. Cadars, V. Prevot, Beilstein J. Nanotechnol. **7**, 2000 (2016)
29. V. Rives, M.A. Ulibarri, Coord. Chem. Rev. **181**, 61 (1999)
30. J. Demel, P. Kubát, I. Jirka, P. Kovář, M. Pospíšil, K. Lang, J. Phys. Chem. C **114**, 16321 (2010)
31. M.R. Islam, Z. Guo, D. Rutman, T.J. Benson, RSC Adv. **3**, 24247 (2013)
32. S. Carlino, Solid State Ionics **98**, 73 (1997)
33. R. Krishnamoorti, I. Banik, L. Xu, Rev. Chem. Eng. **26**, 3 (2010)
34. S.A. Maruyama, S.R. Tavares, A.A. Leitão, F. Wypych, Dyes Pigm. **128**, 158 (2016)
35. R.B. Viana, A.B.F. Da Silva, A.S. Pimentel, Adv. Phys. Chem. **2012**, 1 (2012)
36. A.A. Tsukanov, S.G. Psakhie, Sci. Rep. **6**, 1 (2016)
37. Z. Muda, N. Hashim, I.M. Isa, S. Mustafar, S.A. Bakar, M. Mamat, M.Z. Hussein, Mater. Res. Innov. **00**, 1 (2019)
38. R.A.W. Sing, K.S.W. Everet, D.H. Haul, Pure Appl. Chem. **57**, 603 (1985)
39. S. Hall and K. Jayaraman, Mater. Chem. Phys. (2017)
40. K.C. Ng, M. Burhan, M.W. Shahzad, A.B. Ismail, Sci. Rep. **7**, 1 (2017)
41. R. Nawang, M.Z. Hussein, K.A. Matori, C.A.C. Abdullah, M. Hashim, Results Phys. **15**, 102540 (2019)
42. T. Masuda, N. Fukumoto, M. Kitamura, S.R. Mukai, K. Hashimoto, T. Tanaka, T. Funabiki, Microporous Mesoporous Mater. **48**, 239 (2001)
43. R. Bardestani, G.S. Patience, S. Kaliaguine, Can. J. Chem. Eng. **97**, 2781 (2019)
44. M.R.F. Cerqueira, M.F. Pinto, I.N. Derossi, W.T. Esteves, M.D.R. Santos, M.A.C. Matos, D. Lowinsohn, R.C. Matos, Atmos Pollut. Res. **5**, 253 (2014)
45. S.M.N. Mohsin, T.-Y. Hin, S. Fakurazi, P. Arulselvan, M. Hussein, S. Sarijo, Chem. Cent. J. **7**, 26 (2013)
46. X. Kong, S. Shi, J. Han, F. Zhu, M. Wei, X. Duan, Chem. Eng. J. **157**, 598 (2010)
47. P. Costa, J.M.S. Lobo, Lat. Am. J. Pharm. **34**, 1006 (2015)
48. T. Kodama, Y. Harada, M. Ueda, K.I. Shimizu, K. Shuto, S. Komarneni, Langmuir **17**, 4881 (2001)
49. L. Lv, J. He, M. Wei, D.G. Evans, X. Duan, Water Res. **40**, 735 (2006)
50. N.A. Peppas, J.J. Sahlin, Int. J. Pharm. **57**, 169 (1989)
51. M.Z. Hussein, N.S.S.A. Rahman, S.H. Sarijo, Z. Zainal, Int. J. Mol. Sci. **13**, 7328 (2012)

Synthesis and characterisation of zinc hydroxides nitrates–sodium dodecyl sulphate fluazinam nano hosts for release properties

ORIGINALITY REPORT

13%	5%	13%	2%
SIMILARITY INDEX	INTERNET SOURCES	PUBLICATIONS	STUDENT PAPERS

PRIMARY SOURCES

1	Sharifah Norain Mohd Sharif, Norhayati Hashim, Md Isa Illyas, Suriani Abu Bakar et al. "The Impact of Hygroscopic Chitosan Coating on the Controlled Release Behaviour of Zinc hydroxide nitrate–Sodium Dodecylsulphate–Imidacloprid Nanocomposite", New Journal of Chemistry, 2020 Publication	3%
2	Sharifah Norain Mohd Sharif, Norhayati Hashim, Illyas Md Isa, Suriani Abu Bakar et al. "Controlled release formulation of zinc hydroxide nitrate intercalated with sodium dodecylsulphate and bispyribac anions: A novel herbicide nanocomposite for paddy cultivation", Arabian Journal of Chemistry, 2020 Publication	3%
3	Sharifah Norain Mohd Sharif, Norhayati Hashim, Illyas Md Isa, Suriani Abu Bakar et al. "The effect of swellable carboxymethyl	2%

cellulose coating on the physicochemical stability and release profile of a zinc hydroxide nitrate–sodium dodecylsulphate–imidacloprid", Chemical Physics Impact, 2021
Publication

---

4 Submitted to University of Monastir
Student Paper
2%

---

5 Norhayati Hashim, Sharifah Norain Mohd Sharif, Illyas Md Isa, Shahidah Abdul Hamid et al. "Controlled release formulation of an anti-depression drug based on a L-phenylalanate-zinc layered hydroxide intercalation compound", Journal of Physics and Chemistry of Solids, 2017
Publication
1%

---

6 Zuhailimuna Muda, Norhayati Hashim, Illyas Md Isa, Suriani Abu Bakar et al. "Synthesis and characterization of mesoporous zinc layered hydroxide-isoprocarb nanocomposite", Journal of Saudi Chemical Society, 2018
Publication
1%

---

7 Sheikh Ahmad Izaddin Sheikh Mohd Ghazali, Siti Halimah Sarijo, Mohd Zobir Hussein. "New synthesis of binate herbicide-interleaved anionic clay material: synthesis, characterization and simultaneous controlled-
1%

release properties", Journal of Porous Materials, 2021
Publication

Exclude quotes	On	Exclude matches	< 80 words
Exclude bibliography	On		